

## EppA, a Putative Substrate of DdERK2, Regulates Cyclic AMP Relay and Chemotaxis in *Dictyostelium discoideum*

Songyang Chen and Jeffrey E. Segall\*

Department of Anatomy and Structural Biology, Albert Einstein College of Medicine, 1300 Morris Park Avenue, Bronx, New York 10461

Received 23 December 2005/Accepted 26 April 2006

**The mitogen-activated protein kinase DdERK2 is critical for cyclic AMP (cAMP) relay and chemotaxis to cAMP and folate, but the details downstream of DdERK2 are unclear. To search for targets of DdERK2 in *Dictyostelium discoideum*,  $^{32}\text{PO}_4^{3-}$ -labeled protein samples from wild-type and *Dderk2<sup>-</sup>* cells were resolved by 2-dimensional electrophoresis. Mass spectrometry was used to identify a novel 45-kDa protein, named EppA (ERK2-dependent phosphoprotein A), as a substrate of DdERK2 in *Dictyostelium*. Mutation of potential DdERK2 phosphorylation sites demonstrated that phosphorylation on serine 250 of EppA is DdERK2 dependent. Changing serine 250 to alanine delayed development of *Dictyostelium* and reduced *Dictyostelium* chemotaxis to cAMP. Although overexpression of EppA had no significant effect on the development or chemotaxis of *Dictyostelium*, disruption of the *eppA* gene led to delayed development and reduced chemotactic responses to both cAMP and folate. Both *eppA* gene disruption and overexpression of EppA carrying the serine 250-to-alanine mutation led to inhibition of intracellular cAMP accumulation in response to chemoattractant cAMP, a pivotal process in *Dictyostelium* chemotaxis and development. Our studies indicate that EppA regulates extracellular cAMP-induced signal relay and chemotaxis of *Dictyostelium*.**

Directed cell movement, or chemotaxis, is vital to numerous biological processes and is displayed by many eukaryotic cells, including endothelial cells, neurons, and cells of the immune system. Chemotaxis is strikingly exhibited in the life cycle of the amoeba *Dictyostelium discoideum* (33). Upon starvation, cells move toward cyclic AMP (cAMP) signals and as many as  $10^5$  cells aggregate in  $\sim 8$  h. Responses known to be activated by binding of extracellular cAMP to the plasma membrane cAMP receptor (cAR1) include activation of adenylyl cyclase A (ACA) and guanylyl cyclase, production of phosphatidylinositol phosphates, synthesis of intracellular cAMP and relay of the extracellular cAMP signals, chemotaxis, and expression of development stage genes.

Mitogen-activated protein (MAP) kinase cascades are conserved signaling pathways in eukaryotes for the transfer of extracellular signals to a variety of intracellular regulatory pathways. These sequentially activated kinase cascades are induced by diverse G protein- and tyrosine kinase-coupled receptors. In *Dictyostelium* cells, three components of MAP kinase cascades have been identified. The MAP kinase kinase (MEK) DdMEK1 is required for chemotaxis toward cAMP during aggregation (13). Knockout of DdMEK1 impaired the formation of normal-sized aggregates. However, these small aggregates can still differentiate to form normally proportioned, small fruiting bodies. DdMEK1 is required for activation of guanylyl cyclase and the synthesis of cGMP, a second messenger regulating chemotaxis, in response to extracellular cAMP. There are two MAP kinases, DdERK1 and DdERK2, in *Dictyostelium* cells. Their activity peaks between 15 s and 1 min after stimulation (26, 32). In general, ERKs are proline

directed in that they target substrates that contain a proline in the P+1 site (Ser/Thr-Pro) (23). ERKs are uniformly distributed in the cytoplasm in quiescent cells, but a significant population of ERKs accumulates in the nucleus upon stimulation. Activated ERKs phosphorylate numerous substrates in all cellular compartments, including various nuclear substrates (SRC-1, Pax6, NF-AT, Elk-1, MEF2, c-Fos, c-Myc, and STAT3), membrane proteins (CD120a, Syk, and calnexin), cytoskeletal proteins (neurofilaments and paxillin), and several protein kinases (RSK, MSK, and MNK) (20).

We and others have previously found that DdERK2 contributes to *Dictyostelium* chemotaxis (14, 15, 26, 34). *Dderk2<sup>-</sup>* cells show defects in folate and cAMP chemotaxis and fail to accumulate intracellular cAMP. Identification of a substrate(s) of DdERK2 will enhance our understanding of how DdERK2 regulates chemotaxis. In this study, we identified a new substrate of DdERK2, EppA. DdERK2 regulates phosphorylation of EppA at serine 250, and DdERK2-dependent phosphorylation of EppA is important in regulating directionality, velocity, and persistence during chemotaxis to cAMP. EppA is also required for accumulation of intracellular cAMP.

### MATERIALS AND METHODS

**Maintenance of strains, starvation, radiolabeling of *Dictyostelium*, and cAMP stimulation.** The *Dictyostelium discoideum* axenic strains HS176 (wild type) and HS174 (*Dderk2<sup>-</sup>*) (26) were maintained in HL5 medium (30) in suspension at 170 rpm. Strains expressing myc-tagged forms of EppA were maintained in HL5 supplemented with 10  $\mu\text{g}/\text{ml}$  G418 (Gibco). PCR reagents and restriction enzymes were from Invitrogen (Carlsbad, CA) and Promega (Madison, WI), respectively. The radioisotope  $^{32}\text{PO}_4^{3-}$  used for in vivo labeling was from ICN (Irvine, CA). Starvation buffer consisted of 20 mM 2-(*N*-morpholino)ethanesulfonic acid (MES)-KOH (pH 6.6), 2 mM  $\text{MgCl}_2$ , and 0.2 mM  $\text{CaCl}_2$ . A total of  $5 \times 10^7$  cells were suspended in 10 ml buffer, starved 2 h, and pulsed with 300 nM cAMP every 6 min for 4 h. A total of  $4 \times 10^7$  starved cells were resuspended in 2 ml buffer, mixed with 50  $\mu\text{Ci}$   $^{32}\text{PO}_4^{3-}$ , and shaken for 25 min at 22 to 24°C. Then the cells were stimulated with 10  $\mu\text{M}$  cAMP and folate (Sigma, St. Louis, MO). The stimulated cells were lysed by an equal volume of phenol, and protein pellets were washed with ether.

\* Corresponding author. Mailing address: Department of Anatomy and Structural Biology, Albert Einstein College of Medicine, 1300 Morris Park Ave., Bronx, NY 10461. Phone: (718) 430-4237. Fax: (718) 430-8996. E-mail: segall@aecom.yu.edu.

**2-D electrophoresis.** For isoelectric focusing (IEF), 18-cm precast IPG strips (pI 4 to 7) and an IPGphor IEF unit (Amersham Pharmacia Biotech, Sunnyvale, CA) were used as described elsewhere (8). Three hundred micrograms of protein was focused for 98,000 Vh in a sample buffer containing 6 M urea, 2 M thiourea, 4% 3-[(3-cholamidopropyl)-dimethylammonio]-1-propanesulfonate (CHAPS), 0.5% Pharmalyte (pH 3 to 10), 0.5% Pharmalyte (pH 4 to 7), and 0.4% dithiothreitol. As soon as IEF was finished, the strips were either frozen at  $-70^{\circ}\text{C}$  or equilibrated with buffer (0.375 M Tris-Cl [pH 8.8], 6 M urea, 1% sodium dodecyl sulfate [SDS], and 30% glycerol) containing 1% dithiothreitol or 4% iodoacetamide for 10 min each. Then the second dimension was carried out on 10% SDS-acrylamide gels. After electrophoresis, radioactive 2-dimensional (2-D) gels were stained with colloidal Coomassie brilliant blue (Sigma; 0.5% in 50% methanol–10% acetic acid), wrapped in plastic film, exposed for 1 to 3 days to PhosphorImager screens (Molecular Dynamics, Sunnyvale, CA), and scanned with a Storm 4500 imager (Molecular Dynamics) at a resolution of 100 pixels/cm and a depth of 8 bits. Radioactively labeled filter squares were placed at the corners of the gels for alignment with corresponding Coomassie-stained images using Adobe Photoshop, version 5.5.

**MS analysis of protein.** Excised protein spots were destained and digested as described elsewhere (<http://donatello.ucsf.edu/ingel.html>). The digested peptides were concentrated with  $\text{C}_{18}$  Ziptips (Millipore, Billerica, MA) and placed on matrix-assisted laser desorption/ionization (MALDI) target plates with  $\alpha$ -cyano-4-hydroxycinnamic acid in 50% acetonitrile–1% trifluoroacetic acid. MALDI-time-of-flight (TOF) mass spectrometry (MS) was performed using a Voyager mass spectrometer (Applied Biosystems, Foster City, CA). MS spectra were interpreted using the Data Explore program, version 4.0. Samples from four gels were pooled and submitted to the Rockefeller University Proteomics Resource Center for liquid chromatography-tandem MS (LC-MS/MS) identification. Sequences collected from tryptic peptides were used to search the *Dictyostelium* genomic sequence database.

**Expression constructs of myc-tagged EppA protein and point mutations of serine residues in myc-EppA.** All DNA manipulations were carried out according to standard molecular biology techniques (21). All restriction enzymes were from Promega. The *D. discoideum* genome and cDNA database were searched using amino acid sequences acquired from LC-MS/MS, and as a result, a genomic DNA sequence was found on chromosome 4. Full-length cDNA (clone VFD141) was provided by the Japanese *Dictyostelium* cDNA project, and primers were designed for adding a single myc tag to the full-length cDNA. PCR amplification was performed with primers EppA-5'-myc (5'-GCATGCctgagcaaaagtaactccggaagagcctattcaataaagacaaatcaat-3'); the myc coding sequence is underlined) and EppA-3' (5'-GAGCTCtaaatgattgattgttgat-3'), carrying SphI and SacI restriction enzyme sites (capitalized and italicized), respectively. All PCR amplifications were carried out using the *Pfx* high-fidelity PCR system. The PCR product thus amplified was purified using a QIAquick PCR purification kit (QIAGEN, Valencia, CA), cloned into the pGEM-T plasmid vector (Promega), and sequenced. Then the SphI-SacI fragment was inserted into the pDNeo II plasmid to create a pDNeo II-EppA plasmid vector in which EppA carries an N-terminal myc tag. The insertion was confirmed by sequencing.

To generate point mutations of serine residues in EppA, the pDNeo II-EppA vector was used as a template, and four pairs of primers (S64A [5'-TCATCATCATCTCCGCACCACAAGAAAAGAAA-3' and 5'-TTTCTTTTCTTGTGGTGCGGAGGATGATGATGA-3'], S126A [5'-CAAAGAGGTGAAGATGCAATCTGAAAGAGAT-3' and 5'-ATCTCTTTCAGATGGTGCATCTTCACCTCTTTG-3'], S250A [5'-TTCAGCAATGGTGTGCCCATTCACCACTTCAAG-3' and 5'-CTTGAAGTTGAATGGGCAACACCATTGCTGAA-3'], and S325A [5'-AATCCATTCGGTGGTGGCCCAAGAACTAC-3' and 5'-ATCGTAGTTTCTTGGGGCACCACCGAATGGATT-3']); mutations are underlined) were designed to change serine to alanine using the QuikChange kit (Stratagene, La Jolla, CA) by following the manufacturer's instructions. The DpnI-digested PCR product was used to transform *Escherichia coli* HB101 cells. Plasmids carrying the correct point mutation were confirmed by sequencing.

**Generation of stable cell lines.** Stable *Dictyostelium* cell lines expressing myc-tagged EppA proteins were generated as described previously (19) with the following modifications. HS176 and HS174 cells growing in suspension were collected and electroporated in H-50 buffer by using 10  $\mu\text{g}$  of the above-mentioned plasmid expression vector DNA, and after overnight growth in growth medium, transformants were selected in the presence of 10  $\mu\text{g}/\text{ml}$  G418. Individual colonies were picked after 7 to 10 days and then transferred to 24-well plates, followed by further growth in 10-cm culture plates. Total-cell lysates made from each putative clone were tested for the expression of myc-tagged EppA proteins by performing Western blot analyses with an anti-myc antibody (Upstate, Charlottesville, VA).

**Immunoprecipitation and Western blotting.** HS176 and HS174 stable cell lines expressing myc-tagged EppA protein were grown in suspension. The protocol described above was used for starvation and stimulation. For each sample, 200  $\mu\text{l}$  of cells was lysed in 200  $\mu\text{l}$  of 2 $\times$  radioimmunoprecipitation assay buffer (35) and vortexed for 5 s. The supernatant obtained by centrifugation at high speed in a cold room centrifuge (10 min in a Microfuge at  $\sim 10,000 \times g$ ) was mixed with anti-myc immunoglobulin G (BioMol, Plymouth Meeting, PA) and kept on a rotating shaker for 1 h at  $4^{\circ}\text{C}$ . Protein G-agarose beads (Upstate) were added, and the sample was kept on the rotating shaker for 1 h at  $4^{\circ}\text{C}$ . Then beads were collected by centrifugation at high speed for 10 s. The protein-bound beads were subjected to thorough washing with ice-cold radioimmunoprecipitation assay buffer. After removal of excess washing buffer, protein beads were resuspended in 80  $\mu\text{l}$  2 $\times$  SDS sample buffer and boiled for 5 min.

Western blot analyses were performed as described previously (35) with the following modifications. Cells ( $1 \times 10^7$ ) in MES buffer were lysed by an equal volume of 2 $\times$  SDS sample buffer carrying 1 mM 2-mercaptoethanol and then boiled at  $95^{\circ}\text{C}$  for 5 min. Lysate samples (10  $\mu\text{l}$ ) or immunoprecipitation products (20  $\mu\text{l}$ ) were subjected to electrophoresis on 10% SDS-acrylamide gels and then transferred to nitrocellulose membranes using a Trans-Blot SD semidry transfer cell (Bio-Rad, Hercules, CA) and probed with corresponding antibodies. The anti-ERK2 antibody was made against the *Dictyostelium* protein DdERK2 and detects both unphosphorylated and phosphorylated forms (35). The anti-cAR1 antibody is a gift from P. Devreotes. Signal was detected with corresponding horseradish peroxidase-linked secondary antibodies (Pierce, Rockford, IL) by the PicoWest reagents (Pierce) and chemiluminescence detection system.

**Gene disruption in *Dictyostelium*.** The disruption construct was assembled in plasmid pBsr $\Delta$ BglIII. A 440-bp DNA sequence was PCR amplified using primer 1 (5'-TCTAGAaccagcttcattcattcag-3') and primer 2 (5'-ACTAGTaccattaccataaccac-3') from the N terminus of the *eppA* gene. (The capitalized and italicized bases correspond to XbaI and SpeI restriction sites, respectively.) The purified DNA fragment was cloned as an XbaI/SpeI fragment into the XbaI site of pBsr $\Delta$ BglII to generate the pBsr $\Delta$ BglII-5'-EppA vector. Similarly, another DNA fragment of 626 bp was PCR amplified using primer 3 (5'-AAGCTTACTAGTtcatgttctgttctgttctga-3') with HindIII and SpeI sites and primer 4 (5'-AAGCTTtgctatgttggtaatcgtga-3') with the HindIII site from the C terminus of the *eppA* gene. The purified fragment was digested with HindIII and cloned into the HindIII site of the pBsr $\Delta$ BglII-5'-EppA vector to create the pBsr $\Delta$ BglII-EppA-KO plasmid vector. The SpeI site in primer 3 was used to determine the orientation of the insertion. From this vector DNA, the entire knockout cassette carrying the blasticidin resistance cartridge in the middle was PCR amplified using primers 1 and 4. The amplified PCR DNA was purified and used for electroporation of HS176 cells as described previously (2). Transformants were selected in the presence of 10  $\mu\text{g}/\text{ml}$  blasticidin in the growth medium. Individual clones were isolated, amplified, and subjected to further analyses. Genomic DNA isolated from each clone was analyzed by genomic PCR by using primers 1 and 4.

**Chemotaxis of *Dictyostelium* cells in a Zigmond chamber.** Cells were starved with pulsing as described above for 8 h. cAMP chemotaxis was assayed as described previously (24). In brief, after starvation for 8 h, cells were diluted to  $2 \times 10^5/\text{ml}$  in Ca/Mg phosphate buffer and separated by shearing 20 times with a 200-ml Gilson Pipetman. The cells were then allowed to settle onto an acid-cleaned coverslip for 15 min, and the coverslip was placed on a Zigmond chamber (Neuroprobe, Gaithersburg, MD). The cells were initially followed in the absence of a gradient; then, after 15 to 20 min, a gradient was imposed. Ten minutes after the cAMP gradient was established, cell motility parameters were followed at 10-min intervals for 20 to 30 min. Cell behavior was analyzed with ImageJ. Cell position was measured every 30 s. Theta is defined as the angle between the cAMP gradient and the line connecting the starting and ending centroids every 30 s. The instantaneous velocity is the difference in position between cell centroids in two consecutive frames divided by 30 s. Persistence was calculated by dividing the distance by the path length, where the distance is the difference between the starting centroid and the centroid at 10 min, and the path length is the sum of all centroid differences measured in 30-s intervals. The average for each cell was in further statistical analyses.

**In vivo cAMP production assays.** Cells were starved 2 h in phosphate buffer, pulsed for 4 h, treated with 2.5 mM caffeine for 30 min, washed twice, resuspended in Ca/Mg phosphate buffer to  $5 \times 10^7/\text{ml}$ , and incubated for 5 min at room temperature. Then the cells were stimulated with 10  $\mu\text{M}$  3'-deoxy-cAMP (Sigma). Aliquots of stimulated cells were taken at specific time points, lysed by an equal volume of 3.5% perchloric acid, and neutralized by 50% saturated potassium bicarbonate. The total level of cAMP was measured by a competition assay using an Amersham TRK 432 kit.

**Folate chemotaxis assays.** Axenically grown cells were centrifuged and cells from the pellet dotted on an agar dish containing 1% Bacto agar (Difco, Sparks, MD) in 17 mM phosphate buffer, 1 mM MgCl<sub>2</sub>, and 1 mM CaCl<sub>2</sub>. They were placed 3 to 4 mm from the edge of a well containing 1 mM folate. The positions of the cells were recorded by photographing at the beginning and after 7 to 9 h. The distance of the moving front was measured and used to calculate an average speed of spread. Then the average speeds were converted to the percentage of the speed of wild-type cells. Results are means  $\pm$  standard errors of the means from three experiments.

**Reverse transcription-PCR (RT-PCR) analysis of *eppA* expression.** At different time points during the development at 22°C, total RNA was isolated from HS176 cells by using TRIzol reagent, followed by synthesis of cDNA with random hexamers as primers. Using synthesized cDNA as a template, PCR amplifications were performed with *eppA* gene-specific primers *eppA*(361-382) (5'-G GTAATGCTAGACCAACTGATG-3') and *eppA*(889-865) (5'-CACGATCTT GAGTACCTCTGTAACC-3') to amplify a 528-bp fragment. As a control, the constitutively expressed gene *IG7* (18) was amplified with primer pairs *IG7-S* (5'-TTACATTTATTAGACCCGAAACCAAGCG-3') and *IG7-AS* (5'-TTCCC TTTAGACCTATGGACCTTAGCG-3') on the same template sample.

## RESULTS

**Separation of cAMP-responsive phosphoproteins by 2-D electrophoresis.** To identify substrates of DdERK2, we compared the protein phosphorylation patterns of wild-type and *Dderk2*<sup>-</sup> cells after stimulation with the chemoattractant, cAMP. Cells were starved, labeled with <sup>32</sup>P, stimulated with cAMP for 1 min, and then lysed. Solubilized proteins were separated by 2-D electrophoresis, and phosphorylation was quantitated by a PhosphorImager. In Coomassie brilliant blue-stained gels, there are several hundred protein spots resolved by the 2-D gel. The overall pattern of proteins is similar between wild-type and *Dderk2*<sup>-</sup> cells (Fig. 1A).

A total of 35 phosphorylation spots could be consistently identified (Fig. 1B; Table 1) in the autoradiograms. The majority showed increases in both wild-type (31 out of 35) and *Dderk2*<sup>-</sup> (22 out of 35) cells after cAMP stimulation. Three spots in wild-type cells and 12 spots in *Dderk2*<sup>-</sup> cells showed no change in phosphorylation after cAMP stimulation. Both wild-type and *Dderk2*<sup>-</sup> cells showed one spot with reduced phosphorylation after stimulation. Five spots showed statistically significant ( $P < 0.05$ ) DdERK2-dependent phosphorylation increases (spots 3, 4, 10, 18, and 31).

We then aligned the Coomassie brilliant blue-stained gels with the autoradiographs to identify the corresponding phosphoproteins. Spots 4, 10, 18, and 31 could not be identified—the corresponding protein spot in the Coomassie brilliant blue gel could not be found due to a small amount of protein or was masked by overlapping highly abundant proteins—and thus, these potential substrates have not been further pursued. However, spot 3 had a clear protein in the corresponding Coomassie brilliant blue gel (Fig. 1C) with an estimated molecular size of 45 kDa and will be referred to as EppA (ERK2-dependent phosphoprotein A). In wild-type cells, the phosphorylation intensity of EppA increased 2.95-

fold in response to cAMP, while in *Dderk2*<sup>-</sup> cells, the intensity increased 1.2-fold (Fig. 1C; Table 1). The difference is statistically significant ( $P < 0.01$ ). We therefore focused on this protein as a candidate DdERK2 substrate or downstream effector.

**Identification of EppA.** To identify the potential DdERK2 substrate EppA, the protein was excised from the Coomassie brilliant blue-stained gels and digested with trypsin, and the peptides extracted from the digestion were used for MS/MS sequencing and MALDI-TOF analysis. Upon a search of the *Dictyostelium* genomic database with the MS/MS sequencing results (Table 2), sequence matches with a single 45-kDa open reading frame in expressed sequence tag and genomic databases (7, 17) were identified with high probability. The MALDI-MS spectrum covered 34.6% of the open reading frame, confirming the MS/MS sequencing identification (Fig. 2). The *eppA* gene (DDB0218473) is located on chromosome 4 with one intron. We have not yet found a homologue of EppA in other species. There are four potential ERK phosphorylation sites (Ser/Pro) in the protein (Fig. 2B) and possible evidence for a phosphopeptide containing serine 250 (shown in Fig. 2C).

To confirm that EppA is phosphorylated in vivo, a 10-amino-acid myc tag was added to the N terminus of the open reading frame (Fig. 3A) and the tagged protein was expressed in both wild-type and *Dderk2*<sup>-</sup> cell lines. myc-tagged protein was immunoprecipitated from the cells, and phosphorylation of the protein increased 3.9-fold in wild-type cells after cAMP stimulation, with no change in phosphorylation in *Dderk2*<sup>-</sup> cells (Fig. 3B). This confirmed that EppA phosphorylation was cAMP stimulated and DdERK2 dependent. Analysis of the kinetics of EppA phosphorylation showed that EppA phosphorylation reached a maximum after the maximum of DdERK2 activation, consistent with EppA being a substrate of DdERK2 (Fig. 3C).

To further characterize the phosphorylation sites of EppA, the four potential DdERK2 recognition serine sites in EppA were mutated to alanine individually and reintroduced into wild-type cells. Three point mutants (S64A, S126A, and S325A) showed increased phosphorylation after cAMP stimulation, comparable to that of wild-type EppA protein (Fig. 3D). However, mutation of Ser250 to alanine abolished DdERK2-dependent phosphorylation of EppA in response to cAMP stimulation. In addition, MALDI-TOF analysis showed a pair of peaks consistent with unphosphorylated and phosphorylated forms of a peptide containing Ser250 (Fig. 2C). These data indicate that Ser250 is the major DdERK2-dependent phosphorylation site in EppA.

Expression of *eppA* was also assessed. RT-PCR of a 528-bp fragment of the *eppA* cDNA from total RNA indicated that on the mRNA level there is little alteration during development

FIG. 1. Identification of EppA by 2-D electrophoresis of <sup>32</sup>P-labeled cells. (A) Coomassie brilliant blue-stained 2-D gels of wild-type and *Dderk2*<sup>-</sup> cells before and 1 min after stimulation with cAMP. The box in the wild-type 1-min sample is shown at higher magnification in panel C. Black squares in diagonally opposite corners are filter papers containing <sup>32</sup>P for registration of the autoradiograms in panel B. (B) Autoradiography of 2-D gels in panel A. Phosphoproteins present in three experiments and quantitated in Table 1 are labeled in the autoradiogram of the stimulated wild-type sample. (C) DdERK2-dependent protein position shift and phosphorylation change of EppA. The arrowhead points to the position of phosphorylated EppA (spot 3 in Fig. 1B), and arrows indicate the corresponding position in samples from unstimulated or *Dderk2*<sup>-</sup> cells.

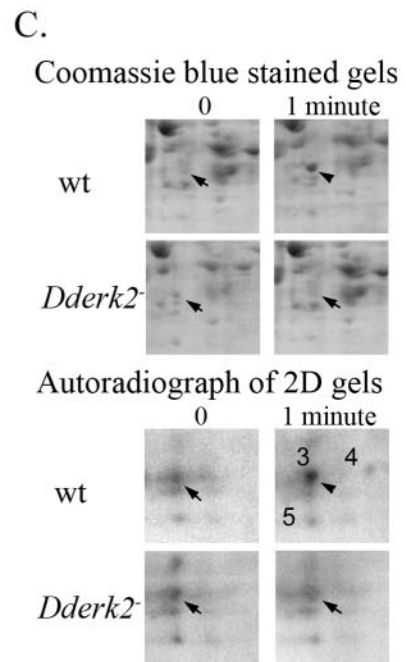
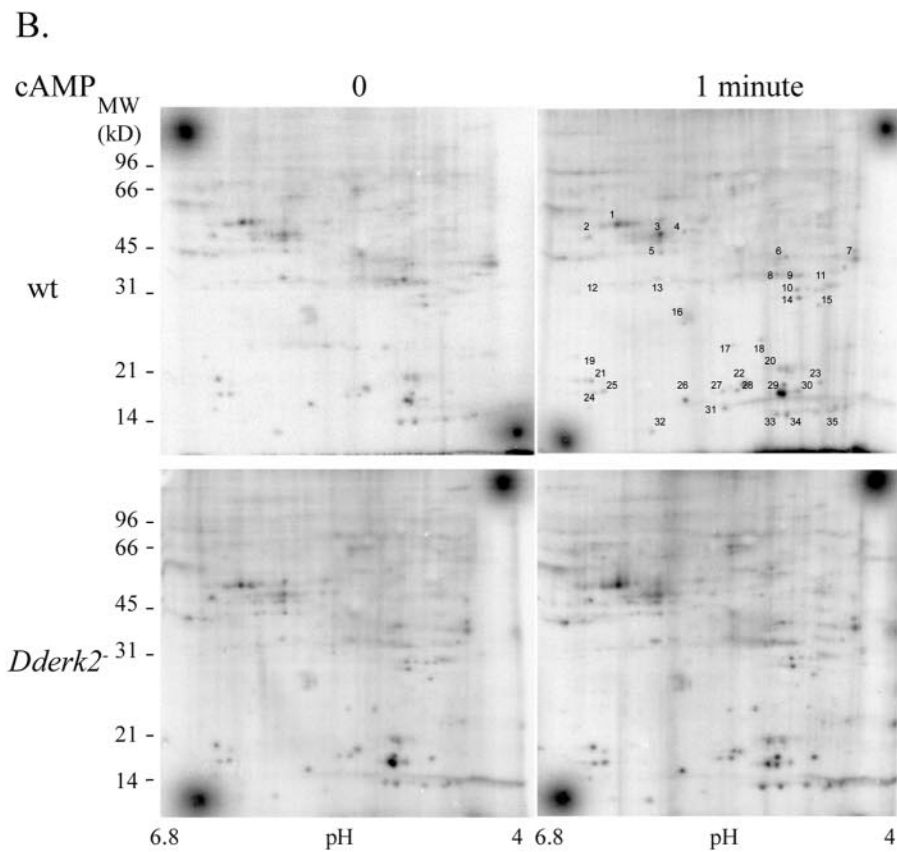
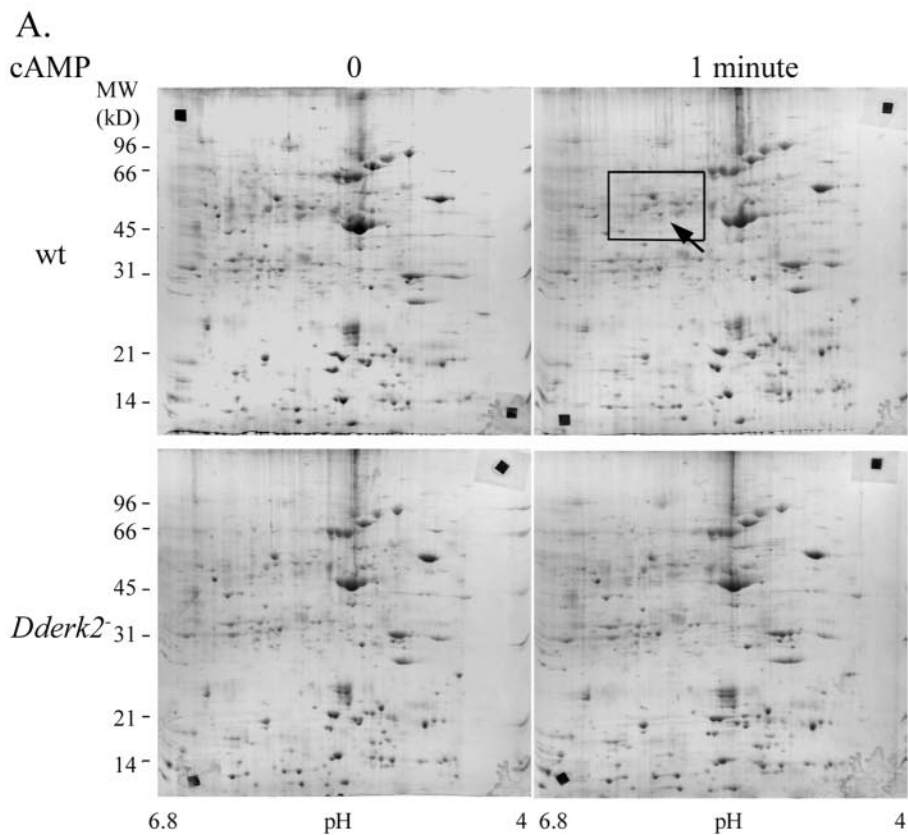


TABLE 1. Comparison of protein phosphorylation changes

Spot no.	Mol mass (kDa)	pI	Relative phosphorylation change (1 min/0 min) <sup>a</sup>		P
			HS176 (ERK2 WT)	HS174 ( <i>erk2</i> <sup>-</sup> )	
1	50	6.3	1.63 ± 0.45	1.54 ± 0.35	0.44
2	44	6.5	2.72 ± 0.95	1.95 ± 0.86	0.29
3	45	5.9	2.95 ± 0.29	1.22 ± 0.06	<0.01
4	46	5.7	2.00 ± 0.39	0.70 ± 0.23	0.02
5	42	5.9	1.59 ± 0.40	2.01 ± 0.78	0.32
6	40	4.8	3.52 ± 1.43	0.91 ± 0.22	0.07
7	40	4.2	0.98 ± 0.37	1.48 ± 0.67	0.28
8	38	4.9	1.94 ± 0.74	1.07 ± 0.43	0.18
9	38	4.7	2.52 ± 0.55	1.22 ± 0.66	0.10
10	36	4.7	3.94 ± 0.71	0.94 ± 0.29	0.01
11	37	4.4	3.61 ± 2.20	0.88 ± 0.22	0.14
12	36	6.6	1.49 ± 0.43	0.96 ± 0.36	0.20
13	38	5.9	0.98 ± 0.34	1.29 ± 0.60	0.34
14	34	4.7	3.82 ± 1.12	1.35 ± 0.57	0.06
15	34	4.5	3.45 ± 1.56	1.43 ± 0.25	0.14
16	30	5.7	1.78 ± 0.41	1.94 ± 0.88	0.44
17	28	5.3	0.78 ± 0.16	1.77 ± 0.74	0.13
18	29	5.0	2.62 ± 0.37	1.33 ± 0.39	0.04
19	27	6.6	0.68 ± 0.40	0.93 ± 0.38	0.34
20	26	4.8	1.89 ± 0.45	1.07 ± 0.11	0.08
21	25	6.5	2.07 ± 0.76	1.11 ± 0.32	0.15
22	24	5.1	2.18 ± 0.75	0.91 ± 0.16	0.09
23	24	4.5	2.85 ± 1.31	2.96 ± 1.86	0.48
24	22	6.5	1.46 ± 0.22	1.02 ± 0.42	0.20
25	22	6.4	1.29 ± 0.23	1.11 ± 0.38	0.35
26	20	5.7	2.06 ± 1.21	1.87 ± 0.84	0.45
27	22	5.3	1.73 ± 0.66	1.16 ± 0.54	0.27
28	22	5.2	2.14 ± 0.98	1.51 ± 0.74	0.32
29	20	4.8	3.20 ± 1.19	1.13 ± 0.23	0.08
30	20	4.7	4.75 ± 1.94	1.45 ± 0.48	0.09
31	18	5.3	2.79 ± 0.45	1.09 ± 0.51	0.03
32	14	6.0	2.43 ± 0.61	1.48 ± 0.90	0.22
33	17	4.9	1.49 ± 0.50	1.25 ± 0.53	0.38
34	17	4.8	1.86 ± 0.69	0.90 ± 0.23	0.13
35	17	4.4	2.65 ± 1.00	0.98 ± 0.20	0.09

<sup>a</sup> <sup>32</sup>P incorporation into spots of 2-D gels was quantified by PhosphorImager and normalized to the protein amount of actin in each gel. Phosphorylation changes of proteins are expressed as the fold change in <sup>32</sup>P incorporation after cAMP stimulation versus before stimulation. Values are means ± standard errors from three experiments. Only proteins that were phosphorylated in three independent experiments were quantified.

(Fig. 4A). *eppA* mRNA expression levels were similar in *Dderk2*<sup>-</sup> mutants (data not shown).

**Disruption of the *eppA* gene causes delayed development and slow growth.** When nutrients are depleted, *Dictyostelium* cells enter a multicellular developmental program leading to the formation of multicellular fruiting bodies and dormant spores. We have previously reported that DdERK2 is required for chemotaxis and morphogenesis in this developmental process (26, 34). To assess the potential role of EppA in *Dictyo-*

TABLE 2. Peptides from EppA sequenced by tandem MS/MS

Peptide	<sup>z</sup> m/z	Sequence
1	<sup>2</sup> 916.8	<sup>69</sup> KVSAPTEDDFPALGQEK
2	<sup>2</sup> 949.3	<sup>51</sup> TYGSQYSSSSSSSPQEK
3	<sup>2</sup> 852.7	<sup>70</sup> VSAPTEDDFPALGQEK
4	<sup>3</sup> 752.8	<sup>27</sup> EKKVSAPTEDDFPALGQEK
5	<sup>2</sup> 712.1	<sup>356</sup> NPSEDVSTNAFNK
6	<sup>2</sup> 596.6	<sup>7</sup> FNLNDLVQTK
7	<sup>2</sup> 908.3	<sup>92</sup> QSQSSSQPPSSGER
8	<sup>2</sup> 622.8	<sup>245</sup> FSNGVSPFNFK
9	<sup>2</sup> 711.3	<sup>5</sup> TKFNLNDLVQTK

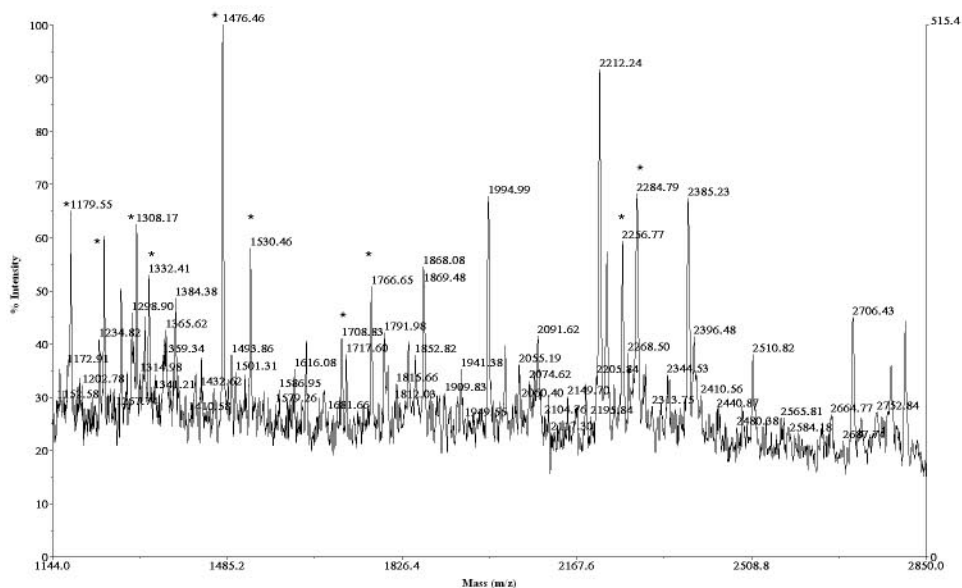
*stelium* development, the expression of EppA in wild-type cells was disrupted via gene targeting with a blasticidin resistance cassette insertion and disruptants identified by genomic PCR as described in Materials and Methods. The effect of the disruption on development on nonnutrient agar was examined. After 24 h, when wild-type cells had formed fruiting bodies, EppA-disrupted cells had just begun to aggregate, and fruiting body formation was delayed (Fig. 4B). Introduction of the myc-tagged *eppA* gene into the EppA-disrupted cells restored fruiting body formation by 24 h. Although overexpression of the myc-tagged full-length EppA in wild-type cells had little effect, overexpression of the Ser250Ala mutation in wild-type cells resulted in a defect similar to that produced by disrupting EppA, consistent with phosphorylation of Ser250 being important for EppA function.

*eppA* disruption also had an effect on cell growth. Wild-type cells divided every 13 h, an interval similar to the 12-h doubling time of the Ax-2 cell line, widely used in *Dictyostelium* studies (Fig. 4C). However, *eppA*-disrupted cells grew significantly more slowly, with a doubling time of 21 h. Reintroduction of myc-EppA into *eppA*<sup>-</sup> cells restored the normal growth rate, with a doubling time of 13.8 h. Mutation of serine 250 or serine 325 also had severe effects on cell growth and increased doubling times to 21 and 27 h, respectively.

**EppA is involved in regulation of *Dictyostelium* chemotaxis.** To determine the function of EppA in *Dictyostelium* chemotaxis, we analyzed responses of wild-type, EppA-overexpressing, and *eppA*<sup>-</sup> cells to an exogenous cAMP gradient. Disruption of the *eppA* gene led to significant decreases in both velocity and chemotaxis (Table 3). These cells also made turns more frequently than wild-type cells (reduced persistence). Introduction of myc-tagged EppA protein into *eppA*<sup>-</sup> cells restored velocity, persistence, and directionality in chemotaxis to cAMP to levels comparable to those of wild-type cells. Expression of EppA in wild-type cells had no significant effect on cell velocity or chemotaxis in a cAMP gradient (Table 3), but expression of the S250A mutant in wild-type cells also

FIG. 2. Identification of EppA by mass spectrometry. (A) MALDI-TOF spectrum of EppA protein. The spot corresponding to phosphorylated EppA was excised and digested with trypsin. The tryptic peptides were extracted and subjected to MALDI-TOF analysis. Peaks that match theoretical tryptic digested peptide masses from EppA are marked by asterisks. (B) Amino acid sequence of EppA. The amino acid sequence was derived from full-length cDNA sequences (clone sVFD141 and AFK 496) provided by the Japanese *Dictyostelium* cDNA project. Four potential Erk2 phosphorylation sites (Ser/Pro) are labeled with asterisks. Amino acids sequenced by LC-MS/MS are boldfaced, and sequences covered by MALDI-TOF are underlined. (C) Mass spectrum of potential phosphopeptide. A portion of panel 2A was enlarged to show a peak (1,244.45 Da) (left arrow) potentially representing the peptide containing serine 250 (amino acids 245 to 255) and the peak (1,323.42 Da) (right arrow) potentially representing the phosphorylated peptide.

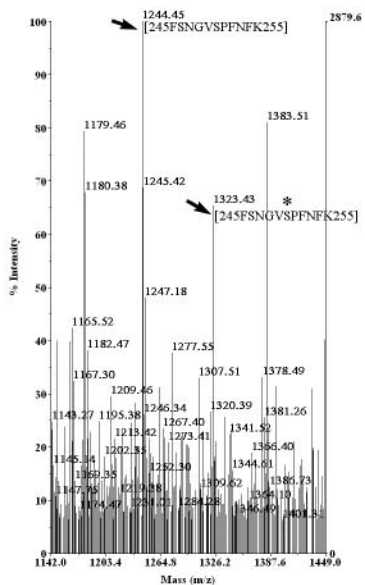
A.



B.

1 MSNKTKFNLN DLVQTKQSSN LPSAPRSSYS EDDENQGGYS GGGYNNRGP TYGSQYSSSS  
 \*  
 61 SSSSPQEKKV SAPTEDDFPA LGQEKPRQP RQQSQSSSQP QPPSSGERVD PFGNARPTDG  
 121 QRGEDSPSER DSEEREERRN DDRYEP RRQQ NDDRDDQDRE GGFNRRGGYNR GGYGGNRDGG  
 \*  
 181 DREGGYNRGG YGGNRDGGDR EGGYRGSYGG GGDREGGYNR GGYGNRDGGD RYNNNRDNR  
 \*  
 241 KDDRFSNGVS PFNFKNNNNR DRDGGDRYNN NRNSGDRDQG GYRGTQDREG GDRYNNNNNR  
 \*  
 301 GGYNRGGYGG NRDGGDRERN PFGGSPRNYD NNRNDRPREE RRPVSKVDS VDDWRNPSED  
 \*  
 361 VSTNAFNKQR KPAPNNNNEQ RSYNNNNNYQ RRDNNEQHDQ QN

C.



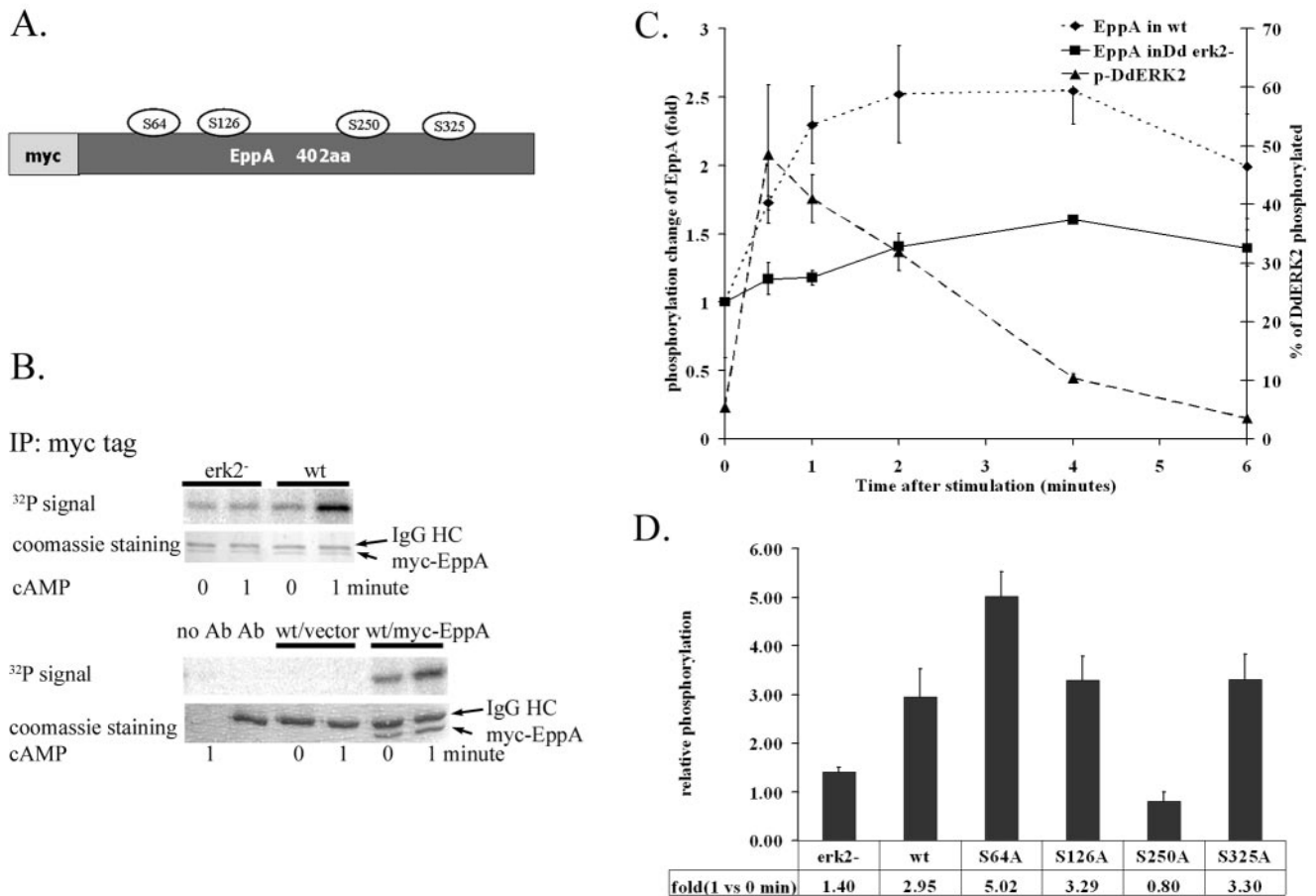


FIG. 3. ERK2-mediated phosphorylation of EppA. (A) myc-tagged EppA construct and putative phosphorylation sites that were mutated. (B) ERK2-dependent *in vivo* phosphorylation of myc-EppA. (Upper panel) myc-EppA was immunoprecipitated from lysates of <sup>32</sup>P-labeled wild-type (wt) or *Dd erk2<sup>-</sup>* (*erk2<sup>-</sup>*) *Dictyostelium* cells stably expressing myc-EppA before and after stimulation with 10  $\mu$ M cAMP. Immunoprecipitates (IP) were separated by SDS-polyacrylamide gel electrophoresis and stained with Coomassie brilliant blue, and phosphorylation was quantitated by a PhosphorImager. (Lower panel) Control to confirm that the lower band is myc-EppA. IgG, immunoglobulin G. (C) Time course of cAMP-induced EppA phosphorylation. Wild-type and *Dd erk2<sup>-</sup>* cells overexpressing myc-tagged EppA were starved 6 h and labeled with <sup>32</sup>PO<sub>4</sub><sup>3-</sup>. myc-tagged EppA was immunoprecipitated from lysates prepared at different time points after cAMP stimulation. The phosphorylation level at each time point was standardized by the amount of myc-EppA. Phosphorylation of DdERK2 after cAMP stimulation was detected by Western blotting, and the densities of corresponding bands were measured and used to determine the percentage of DdERK2 phosphorylated. Values are averages from two experiments. Error bars indicate the range of the original data. (D) Identification of phosphorylation sites. Cells stably expressing myc-EppA constructs carrying the single point mutations identified in panel A were labeled and stimulated, and the myc-tagged protein was immunoprecipitated for SDS-polyacrylamide gel electrophoretic analysis as for panel B. The <sup>32</sup>P signal was normalized to myc-EppA protein staining, and the relative change in EppA phosphorylation (<sup>32</sup>P density of stimulated sample/density of unstimulated sample) was averaged from three to four experiments.

significantly reduced the directionality of cells in the cAMP gradient, with moderate inhibition of velocity and persistence (Table 3). These results suggest that EppA is important in regulating *Dictyostelium* chemotaxis and that ERK2-mediated phosphorylation of serine 250 is required for appropriate chemotaxis.

To evaluate the developmental stage of the cells during the cAMP chemotaxis assay, the expression of *cAR1*, an early developmental marker, was examined. *eppA<sup>-</sup>* cells showed *cAR1* regulation similar to that of wild-type cells (Fig. 4D). Expression of *cAR1* was first seen at 4 h after the onset of starvation and continued to increase, peaking at 6 h, indicating that disruption of *eppA* did not change gene expression in early developmental stages. Thus, the reduced chemotactic response

TABLE 3. Quantitation of cAMP chemotaxis<sup>a</sup>

Strain (n) <sup>b</sup>	Avg cos $\theta$ <sup>c</sup>	Avg velocity ( $\mu$ m/min) <sup>c</sup>	Persistence <sup>c</sup>
wt/pBsr (853)	0.49 $\pm$ 0.01	6.31 $\pm$ 0.39	0.64 $\pm$ 0.03
<i>eppA<sup>-</sup></i> (424)	0.29 $\pm$ 0.04**	4.46 $\pm$ 0.35*	0.55 $\pm$ 0.01*
<i>eppA<sup>-</sup>/myc-EppA</i> (941)	0.56 $\pm$ 0.02	6.67 $\pm$ 0.26	0.69 $\pm$ 0.03
wt (638)	0.58 $\pm$ 0.04	6.41 $\pm$ 0.71	0.73 $\pm$ 0.05
wt/vector (602)	0.62 $\pm$ 0.02	6.17 $\pm$ 0.75	0.75 $\pm$ 0.03
wt/myc-EppA (925)	0.58 $\pm$ 0.01	6.29 $\pm$ 0.16	0.75 $\pm$ 0.01
wt/myc-EppA(S250A) (506)	0.36 $\pm$ 0.06*	5.75 $\pm$ 0.48	0.61 $\pm$ 0.02

<sup>a</sup> Cell chemotaxis was measured on 8-h-starved cells in a Zigmond chamber with a 2  $\mu$ M cAMP gradient.

<sup>b</sup> wt, wild type; n, total number of cells analyzed in three experiments.

<sup>c</sup> Data are means  $\pm$  standard errors from three experiments. \*, *P* < 0.05; \*\*, *P* < 0.01.

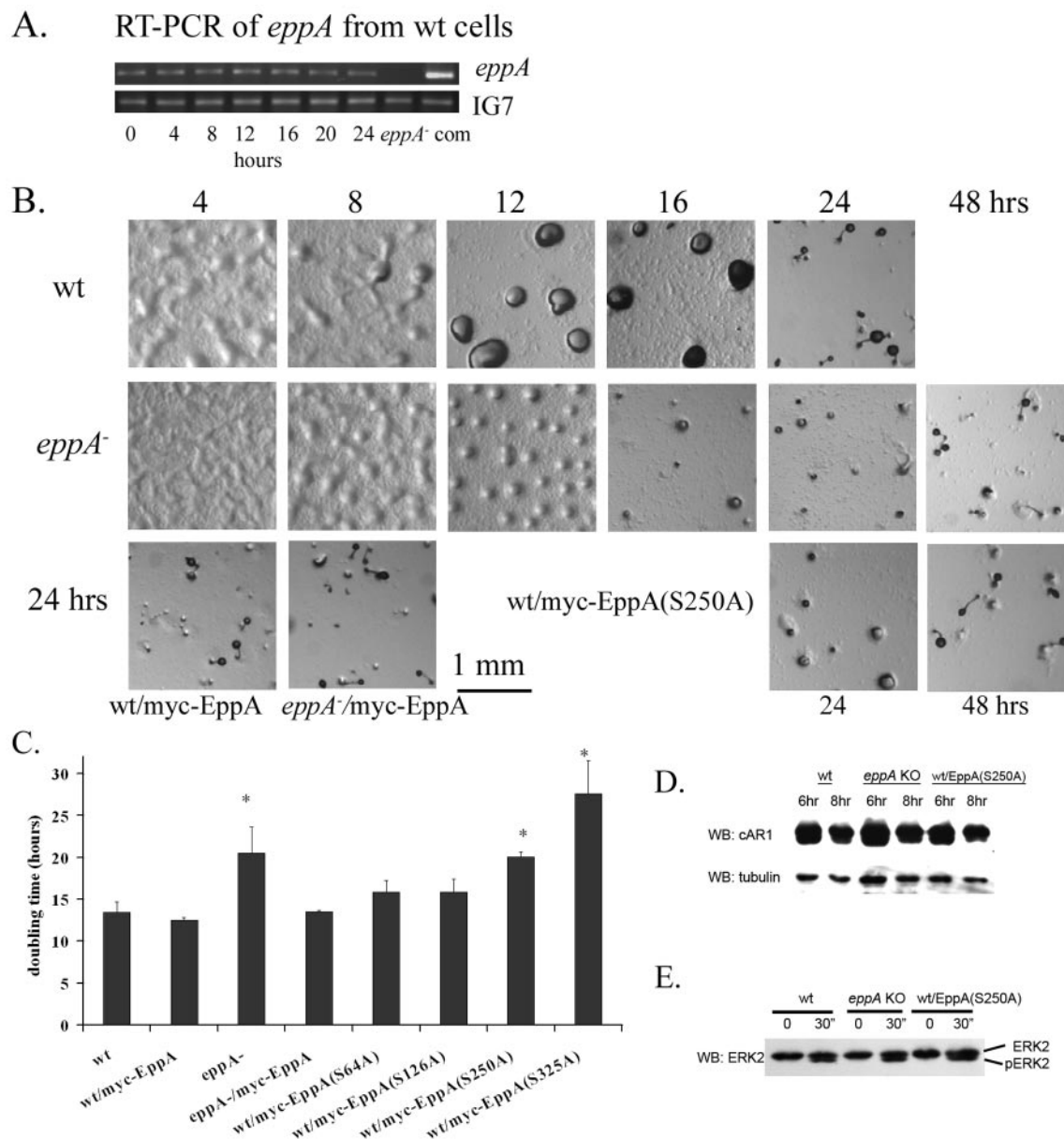


FIG. 4. Disruption of the *eppA* gene and evaluation of development and growth of *Dictyostelium* cells. (A) Expression of the *eppA* gene during development. Wild-type cells (HS176) growing in suspension culture were collected by centrifugation, followed by a wash with phosphate buffer. The cell pellet was resuspended in the buffer, and  $1 \times 10^7$  cells (in 1 ml buffer) were placed on top of Ca/Mg-phosphate agar plates. RNA was isolated at the indicated times. RT-PCR was performed with *eppA*-specific primers after generation of first-strand cDNA by reverse transcriptase. PCR mixtures were subjected to electrophoresis on a 1% agarose gel. As mentioned in Materials and Methods, IG7 is a control constitutively expressed gene. com is an *eppA*<sup>-</sup> disruptant completed by myc-EppA. (B) EppA is required for normal *Dictyostelium* development. A total of  $10^6$  cells in 100  $\mu$ l of phosphate buffer were placed on phosphate agar plates, and cells were allowed to develop at 22°C in a moist chamber. Pictures were taken at the indicated times. Bar, 1 mm. wt, wild-type parental cells; *eppA*<sup>-</sup>, cells with the *eppA* gene disrupted by targeting construct; wt/myc-EppA, wild-type cells overexpressing myc-EppA; wt/myc-EppA(S250A), wild-type cells overexpressing myc-EppA carrying the S250A point mutation; *eppA*<sup>-</sup>/myc-EppA, *eppA* knockout cells expressing myc-EppA. (C) Effect of EppA on *Dictyostelium* cell growth. Cells were grown in suspension, and the doubling time was calculated from cell density measurements made during the exponential-growth phase. Results are means  $\pm$  standard errors of the means from three experiments. (D) Expression of cAR1 in early development of *Dictyostelium*. Cells were starved in PB and pulsed with 100 nM cAMP for varying times after 2 h of starvation. Aliquots of cells were taken at different time points, lysed by 2 $\times$  SDS sample buffer, and Western blotted (WB) with an anti-cAR1 antibody. (E) cAMP-dependent activation of DdERK2. Cells were starved and pulsed for 7 h, treated with caffeine for 10 min, stimulated with 10  $\mu$ M cAMP, lysed by an equal volume of 2 $\times$  SDS sample buffer at 0 and 30 s after stimulation, and Western blotted with an anti-DdERK2 antibody. After stimulation, a higher-mobility band indicates the activated DdERK2 protein under these gel electrophoresis conditions.



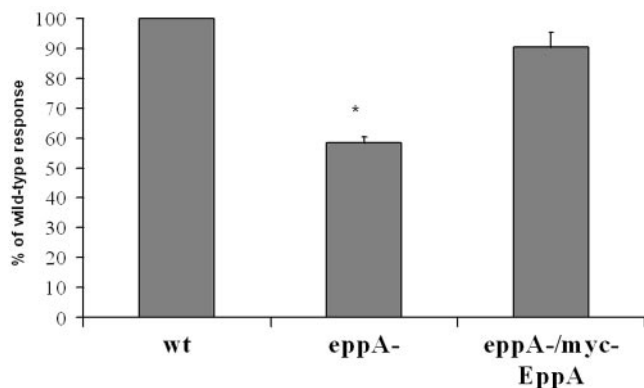


FIG. 5. Quantitation of folate chemotaxis. As many as  $10^6$  cells were placed on an agar surface 3 to 4 mm away from a well containing 1 mM folate, and the migration rate measured as described in Materials and Methods. Data are means and standard errors from three experiments. \*,  $P < 0.05$ .

to cAMP of *eppA*<sup>-</sup> cells indicates a role for EppA in chemotaxis. Expression and activation of DdERK2 were also tested. Wild-type and *eppA*<sup>-</sup> cells expressed similar amounts of DdERK2, and DdERK2 was phosphorylated 30 s after cAMP stimulation (Fig. 4E) in all strains, indicating that upstream signaling and activation of ERK2 were not affected by the loss of EppA function. To determine whether EppA is generally required for chemotaxis or selectively affects cAMP responses, chemotaxis to folic acid was studied using the agar well assay. *eppA*<sup>-</sup> cells responded to folate, but not as efficiently as wild-type cells, suggesting that EppA is required for both cAMP and folate chemotaxis (Fig. 5).

**Regulation of cAMP accumulation by EppA.** Previous studies have demonstrated that DdERK2 activity is required for cAMP accumulation and signal relay (14, 26). Therefore, we tested the role of EppA in intracellular synthesis of cAMP. In contrast to wild-type cells, *eppA*<sup>-</sup> cells displayed only a weak and short increase in cAMP production after stimulation with the cAR1 agonist 2'-deoxy-cAMP (Fig. 6). Expression of myc-EppA in disruptants restored stimulation of cAMP. Expression of the S250A EppA protein in wild-type cells reduced cAMP accumulation to the level of EppA disruptants.

## DISCUSSION

In this study we used 2-dimensional electrophoresis to look for proteins that were phosphorylated by DdERK2 in response to the chemoattractant cAMP. We detected five proteins that showed DdERK2-dependent phosphorylation. By LC-MS/MS and MALDI-TOF, we were able to identify one of them and have named it EppA. The EppA gene is located on chromosome 4, and there is one intron in the genomic sequence. We have found that phosphorylation of EppA on serine 250 is dependent on DdERK2 activity. In *eppA*<sup>-</sup> cells, extracellular cAMP-stimulated accumulation of intracellular cAMP was inhibited. Disruption of the *eppA* gene also led to a deficiency in chemotaxis to cAMP and folate. EppA is required for proper development of *Dictyostelium*.

For aggregation-stage *Dictyostelium* cells, binding of cAMP to the plasma membrane receptor cAR1 triggers a series of

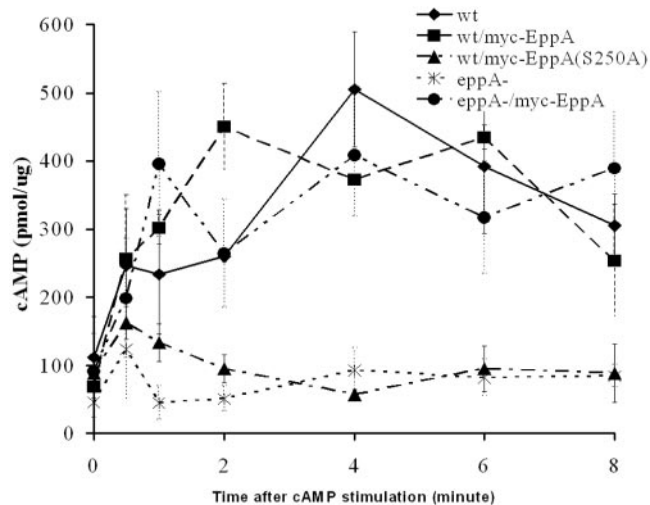


FIG. 6. EppA regulates intracellular cAMP accumulation. Aliquots of cells were lysed at different times before and after stimulation with 5  $\mu$ M 2'-deoxy-cAMP, and intracellular cAMP concentrations were measured. Data are means and standard errors from three or four experiments.

downstream events involving DdERK2. DdERK2 is activated by stimulation of cells with cAMP, and its kinase activity peaks between 30 s and 1 min after cAMP binding to the receptor. DdERK2 is important for accumulation of intracellular cAMP. Two minutes after binding of cAMP to the receptor cAR1, DdERK2 activity begins to drop; it returns to basal levels after 5 min. Before the identification of EppA, the only ERK2 substrate in *Dictyostelium* that had been proposed was RegA, a phosphodiesterase that degrades cAMP specifically (27, 28, 31). It has been proposed that upon stimulation of cells with cAMP, inhibition of RegA activity results in increased intracellular cAMP levels (16). Cells with a disruption of *regA* accumulated more cAMP than wild-type *Dictyostelium* cells in response to cAMP stimulation. *regA* disruptants suppress the defect in aggregation and cAMP production of *Dderk2*<sup>-</sup> mutants, and control of RegA activity may be due to DdERK2-dependent phosphorylation (16). There are four potential DdERK2 recognition sites in RegA, including threonine 676. Expression of RegA protein carrying a mutation of threonine 676 blocks the stimulated production of intracellular cAMP (16). Although threonine 676 is important for the regulation of RegA, there is no direct evidence of phosphorylation of RegA at threonine 676.

We describe here the identification and characterization of EppA as a novel substrate of DdERK2, which regulates chemotaxis and development of *Dictyostelium* cells. cAMP-induced and DdERK2-dependent phosphorylation of EppA was first found by comparing 2-D gels of wild-type and *Dderk2*<sup>-</sup> samples. MS/MS analysis of the protein excised from 2-D gels provided sequences of nine peptides, which covered 29.6% of the EppA coding sequence. Ten peaks in the MALDI-TOF spectrum of tryptic peptides from EppA matched theoretical digestion of the protein and showed a good coverage of EppA. Immunoprecipitation of myc-tagged EppA from wild-type cells displayed a threefold increase in EppA phosphorylation after cAMP stimulation, while *Dderk2*<sup>-</sup> cells showed only a

slight increase, confirming that EppA is phosphorylated by a DdERK2-dependent pathway. Disruption of the *eppA* gene decreased the growth rate and caused delayed development of *Dictyostelium* cells, and the disruptants formed smaller fruiting bodies. The disruptants showed significantly reduced cAMP-stimulated cAMP production, which could delay aggregation kinetics. In addition, in the Zigmond chamber assay, *eppA*<sup>-</sup> cells showed a significant decrease in directionality in a cAMP gradient. Cell velocity and persistence also dropped significantly. The combination of reduced cAMP production and reduced chemotactic response is consistent with the delayed aggregation that is observed. DdERK2 was properly activated by cAMP stimulation in *eppA*<sup>-</sup> cells, indicating that the disruptants were able to develop to the aggregation-competent state and that the major function of EppA is downstream of DdERK2. In addition to chemotaxis to cAMP, EppA disruptants were defective in folate chemotaxis, implying that EppA is required for both cAMP and folate chemotaxis, within the qualitative resolution of the folate chemotaxis assay that was used.

EppA has four potential DdERK2 phosphorylation sites. Mutation of serine 250 to alanine impaired DdERK2-dependent phosphorylation of EppA in response to cAMP stimulation, indicating that serine 250 is required for DdERK2-dependent phosphorylation of EppA. We did not detect DdERK2 coimmunoprecipitated with myc-EppA, implying that DdERK2 interactions with EppA must be relatively brief. Alternatively, it is possible that phosphorylation of EppA at serine 250 is performed by another kinase that is in turn activated by DdERK2. While expression of wild-type EppA in wild-type cells had no effect on any of the phenotypes we have measured, expression of the S250A mutant of EppA in wild-type cells (S250A/EppA) caused a delay in development, consistent with phosphorylation of EppA being important for signaling during development. When we looked at chemotaxis and signal relay, EppA/S250A cells showed decreased directionality, velocity, and persistence in cAMP gradients and lower intracellular cAMP accumulation. These data suggest that the S250A mutant may be a dominant-negative form of EppA, raising the possibility that EppA forms a complex with downstream components that is altered by phosphorylation of EppA.

The precise mechanism(s) by which EppA regulates cAMP synthesis and chemotaxis is still unclear. With respect to cAMP synthesis, EppA may act directly on RegA or in parallel. Although RegA has a potential phosphorylation site (threonine 676) and mutation of the threonine impairs DdERK2-dependent inhibition of RegA (16), there is no direct evidence that RegA is phosphorylated at that site. Thus, it is formally possible that ERK2 phosphorylates EppA and EppA regulates inhibition of RegA in cAMP-stimulated cells. Alternatively, EppA may act in parallel with RegA to control cyclase activity. The regulatory mechanism of ACA activity is complex (22). It is known that CRAC (cytosolic regulator of adenylyl cyclase) (5, 6, 25), RasC (12), Rip3 (10), RasGEF (9), and Pia (4) are required for activation of ACA. How these proteins interact with each other and ACA is unclear. For the adaptation of ACA, Gα9 was found to have an inhibitory effect on ACA (3). Since Gα9-null cells still showed periodic signaling, there must be other mechanisms to negatively regulate ACA.

With respect to the reduction in chemotaxis, the defects in EppA disruptants may be due to the alteration in intracellular cAMP. Proper accumulation and degradation of cAMP is important for protein kinase A function and inhibition of lateral pseudopod formation in chemotaxis (29). Mutants lacking ACA have reduced chemotactic responses in cAMP gradients, and thus, the reduced cAMP production in *eppA*<sup>-</sup> cells could result in a phenotype similar to that of *aca*<sup>-</sup> mutants.

The sequence of EppA does not show strong homologies to other proteins, as is also true for CRAC, another regulator of adenylyl cyclase (11). The presence of strings of arginines and a repeated motif involving glycine can be seen in DNA and RNA binding proteins, but sequence searches have not identified a standard DNA or RNA binding domain. Thus, it is possible that EppA is also involved in regulation of transcription or translation. The glycine-rich domain of TAFII68 has been shown to interact with the DNA binding domain in *cis* or in *trans* (1), and thus, EppA's glycine-rich domain may also play a role in intramolecular or intermolecular interactions. The myc-tagged EppA construct, which fully restores chemotaxis and development in the EppA disruptants, is mainly cytoplasmic and not localized to the nucleus. Thus, we currently favor models focusing on a cytoplasmic function for EppA.

In summary, we have identified a novel protein, EppA, whose phosphorylation is regulated by DdERK2 and which is necessary for chemotaxis to cAMP and intracellular production of cAMP. We have identified the DdERK2-dependent phosphorylation site on EppA and shown that mutating this site to alanine generates a dominant-negative form, demonstrating that phosphorylation is important in the regulation of EppA. Identification of the interacting partners of EppA will aid in determining the mechanism of action of EppA in the regulation of cAMP production and chemotaxis.

#### ACKNOWLEDGMENTS

We thank P. Devreotes for providing the anti-cAR1 antibody, R. Gomer for providing the pBsr3ΔBgIII plasmid, and H. Urushihara and the Japanese *Dictyostelium* cDNA project for providing the full-length cDNA of EppA. We also thank R. Angeletti and E. Neves for help on MALDI-TOF analysis and J. Chubb for help on establishing knockout strains. We appreciate the suggestion of EppA as the name for p45 from a reviewer.

This work was supported by MCB9728324 and CA100324.

#### REFERENCES

- Alex, D., and K. A. Lee. 2005. RGG-boxes of the EWS oncoprotein repress a range of transcriptional activation domains. *Nucleic Acids Res.* **33**:1323–1331.
- Betapudi, V., K. Shoebtham, and T. T. Egelhoff. 2004. Generation of double gene disruptions in *Dictyostelium discoideum* using a single antibiotic marker selection. *BioTechniques* **36**:106–112.
- Brzostowski, J. A., C. Johnson, and A. R. Kimmel. 2002. Gα-mediated inhibition of developmental signal response. *Curr. Biol.* **12**:1199–1208.
- Chen, M. Y., Y. Long, and P. N. Devreotes. 1997. A novel cytosolic regulator, Pianissimo, is required for chemoattractant receptor and G protein-mediated activation of the 12 transmembrane domain adenylyl cyclase in *Dictyostelium*. *Genes Dev.* **11**:3218–3231.
- Comer, F. I., C. K. Lippincott, J. J. Masbad, and C. A. Parent. 2005. The PI3K-mediated activation of CRAC independently regulates adenylyl cyclase activation and chemotaxis. *Curr. Biol.* **15**:134–139.
- Dormann, D., G. Weijer, C. A. Parent, P. N. Devreotes, and C. J. Weijer. 2002. Visualizing PI3 kinase-mediated cell-cell signaling during *Dictyostelium* development. *Curr. Biol.* **12**:1178–1188.
- Eichinger, L., J. A. Pachebat, G. Glockner, M. A. Rajandream, R. Suggang, M. Berriman, J. Song, R. Olsen, K. Szafranski, Q. Xu, B. Tunggal, S. Kummerfeld, M. Madera, B. A. Konfortov, F. Rivero, A. T. Bankier, R. Lehmann, N. Hamlin, R. Davies, P. Gaudet, P. Fey, K. Pilcher, G. Chen, D.

- Saunders, E. Sodergren, P. Davis, A. Kerhornou, X. Nie, N. Hall, C. Anjard, L. Hemphill, N. Bason, P. Farbrother, B. Desany, E. Just, T. Morio, R. Rost, C. Churcher, J. Cooper, S. Haydock, N. van Driessche, A. Cronin, I. Goodhead, D. Muzny, T. Mourier, A. Pain, M. Lu, D. Harper, R. Lindsay, H. Hauser, K. James, M. Quiles, M. Madan Babu, T. Saito, C. Buchrieser, A. Wardroper, M. Felder, M. Thangavelu, D. Johnson, A. Knights, H. Loulseged, K. Mungall, K. Oliver, C. Price, M. A. Quail, H. Urushihara, J. Hernandez, E. Rabinowitsch, D. Steffen, M. Sanders, J. Ma, Y. Kohara, S. Sharp, M. Simmonds, S. Spiegler, A. Tivey, S. Sugano, B. White, D. Walker, J. Woodward, T. Winckler, Y. Tanaka, G. Shaulsky, M. Schleicher, G. Weinstock, A. Rosenthal, E. C. Cox, R. L. Chisholm, R. Gibbs, W. F. Loomis, M. Platzer, R. R. Kay, J. Williams, P. H. Dear, A. A. Noegel, B. Barrell, and A. Kuspa. 2005. The genome of the social amoeba *Dictyostelium discoideum*. *Nature* **435**:43–57.
8. Hermann, T., M. Finkemeier, W. Pfefferle, G. Wersch, R. Kramer, and A. Burkovski. 2000. Two-dimensional electrophoretic analysis of *Corynebacterium glutamicum* membrane fraction and surface proteins. *Electrophoresis* **21**:654–659.
  9. Insall, R. H., J. Borleis, and P. N. Devreotes. 1996. The aimless RasGEF is required for processing of chemotactic signals through G-protein-coupled receptors in *Dictyostelium*. *Curr. Biol.* **6**:719–729.
  10. Lee, S., C. A. Parent, R. Insall, and R. A. Firtel. 1999. A novel Ras-interacting protein required for chemotaxis and cyclic adenosine monophosphate signal relay in *Dictyostelium*. *Mol. Biol. Cell* **10**:2829–2845.
  11. Lilly, P. J., and P. N. Devreotes. 1994. Identification of CRAC, a cytosolic regulator required for guanine nucleotide stimulation of adenylyl cyclase in *Dictyostelium*. *J. Biol. Chem.* **269**:14123–14129.
  12. Lim, C. J., G. B. Spiegelman, and G. Weeks. 2001. RasC is required for optimal activation of adenylyl cyclase and Akt/PKB during aggregation. *EMBO J.* **20**:4490–4499.
  13. Ma, H., M. Gamper, C. Parent, and R. A. Firtel. 1997. The *Dictyostelium* MAP kinase kinase DdMEK1 regulates chemotaxis and is essential for chemoattractant-mediated activation of guanylyl cyclase. *EMBO J.* **16**:4317–4332.
  14. Maeda, M., L. Aubry, R. Insall, C. Gaskins, P. N. Devreotes, and R. A. Firtel. 1996. Seven helix chemoattractant receptors transiently stimulate mitogen-activated protein kinase in *Dictyostelium*. Role of heterotrimeric G proteins. *J. Biol. Chem.* **271**:3351–3354.
  15. Maeda, M., and R. A. Firtel. 1997. Activation of the mitogen-activated protein kinase ERK2 by the chemoattractant folic acid in *Dictyostelium*. *J. Biol. Chem.* **272**:23690–23695.
  16. Maeda, M., S. Lu, G. Shaulsky, Y. Miyazaki, H. Kuwayama, Y. Tanaka, A. Kuspa, and W. F. Loomis. 2004. Periodic signaling controlled by an oscillatory circuit that includes protein kinases ERK2 and PKA. *Science* **304**:875–878.
  17. Morio, T., H. Urushihara, T. Saito, Y. Ugawa, H. Mizuno, M. Yoshida, R. Yoshino, B. N. Mitra, M. Pi, T. Sato, K. Takemoto, H. Yasukawa, J. Williams, M. Maeda, I. Takeuchi, H. Ochiai, and Y. Tanaka. 1998. The *Dictyostelium* developmental cDNA project: generation and analysis of expressed sequence tags from the first-finger stage of development. *DNA Res.* **5**:335–340.
  18. Nagasaki, A., G. Itoh, S. Yumura, and T. Q. Uyeda. 2002. Novel myosin heavy chain kinase involved in disassembly of myosin II filaments and efficient cleavage in mitotic *Dictyostelium* cells. *Mol. Biol. Cell* **13**:4333–4342.
  19. Pang, K. M., M. A. Lynes, and D. A. Knecht. 1999. Variables controlling the expression level of exogenous genes in *Dictyostelium*. *Plasmid* **41**:187–197.
  20. Roux, P. P., and J. Blenis. 2004. ERK and p38 MAPK-activated protein kinases: a family of protein kinases with diverse biological functions. *Microbiol. Mol. Biol. Rev.* **68**:320–344.
  21. Sambrook, J., and D. W. Russell. 2001. *Molecular cloning: a laboratory manual*, 3rd ed. Cold Spring Harbor Laboratory Press, Cold Spring Harbor, N.Y.
  22. Saran, S., M. E. Meima, E. Alvarez-Curto, K. E. Weening, D. E. Rozen, and P. Schaap. 2002. cAMP signaling in *Dictyostelium*. Complexity of cAMP synthesis, degradation and detection. *J. Muscle Res. Cell Motil.* **23**:793–802.
  23. Schaeffer, H. J., and M. J. Weber. 1999. Mitogen-activated protein kinases: specific messages from ubiquitous messengers. *Mol. Cell. Biol.* **19**:2435–2444.
  24. Segall, J. E. 1992. Behavioral responses of streamer F mutants of *Dictyostelium discoideum*: effects of cyclic GMP on cell motility. *J. Cell Sci.* **101**:589–597.
  25. Segall, J. E. 1999. Cell polarization: chemotaxis gets CRACKing. *Curr. Biol.* **9**:R46–R48.
  26. Segall, J. E., A. Kuspa, G. Shaulsky, M. Ecke, M. Maeda, C. Gaskins, R. A. Firtel, and W. F. Loomis. 1995. A MAP kinase necessary for receptor-mediated activation of adenylyl cyclase in *Dictyostelium*. *J. Cell Biol.* **128**:405–413.
  27. Shaulsky, G., R. Escalante, and W. F. Loomis. 1996. Developmental signal transduction pathways uncovered by genetic suppressors. *Proc. Natl. Acad. Sci. USA* **93**:15260–15265.
  28. Shaulsky, G., D. Fuller, and W. F. Loomis. 1998. A cAMP-phosphodiesterase controls PKA-dependent differentiation. *Development* **125**:691–699.
  29. Stepanovic, V., D. Wessels, K. Daniels, W. F. Loomis, and D. R. Soll. 2005. Intracellular role of adenylyl cyclase in regulation of lateral pseudopod formation during *Dictyostelium* chemotaxis. *Eukaryot. Cell* **4**:775–786.
  30. Sussman, M. 1987. Cultivation and synchronous morphogenesis of *Dictyostelium* under controlled experimental conditions. *Methods Cell Biol.* **28**:9–29.
  31. Thomason, P. A., D. Traynor, G. Cavet, W. T. Chang, A. J. Harwood, and R. R. Kay. 1998. An intersection of the cAMP/PKA and two-component signal transduction systems in *Dictyostelium*. *EMBO J.* **17**:2838–2845.
  32. van Es, S., and P. N. Devreotes. 1999. Molecular basis of localized responses during chemotaxis in amoebae and leukocytes. *Cell. Mol. Life Sci.* **55**:1341–1351.
  33. Van Haastert, P. J., and P. N. Devreotes. 2004. Chemotaxis: signalling the way forward. *Nat. Rev. Mol. Cell Biol.* **5**:626–634.
  34. Wang, Y., J. Liu, and J. E. Segall. 1998. MAP kinase function in amoeboid chemotaxis. *J. Cell Sci.* **111**:373–383.
  35. Wang, Y., and J. E. Segall. 1998. The *Dictyostelium* MAP kinase DdERK2 functions as a cytosolic protein in complexes with its potential substrates in chemotactic signal transduction. *Biochem. Biophys. Res. Commun.* **244**:149–155.